Shell model test of quadrupole properties predicted by the rotational formula—the degenerate SDI interaction and non-degenerate FPD6

A. Escuderos and L. Zamick

Department of Physics and Astronomy,

Rutgers University, Piscataway, New Jersey 08854

Abstract

In the rotational model for a $K = 0$ band in an even–even nucleus, there is a single parameter—Q_0, the intrinsic quadrupole moment. All $B(E2)$'s in the band and all static quadrupole moments are expressed in terms of this one parameter. In shell-model calculations, this does not have to be the case. In this work, we consider ground-state bands in ^{44}Ti, ^{46}Ti, ^{48}Ti, ^{48}Cr, and ^{50}Cr with two different models. First, we use a Surface Delta Interaction with degenerate single-particle energies (SDI-deg). We compare this with results of a shell-model calculation using the standard interaction FPD6 and include the single-particle energy splitting. Neither model yields a perfect rotational $I(I + 1)$ spectrum, although the SDI-deg model comes somewhat closer. Overall, the simple rotational formula for $B(E2)$'s and static quadrupole moments hangs together very nicely.

I. INTRODUCTION

In a previous publication [1], we considered the relationship between the static quadrupole moments of the 2_1^+ states and the corresponding $B(E2)$'s in the sd and fp shells. We used the shell model to operationally define a ratio of intrinsic quadrupole moments $Q_0(S)/Q_0(B)$, where $Q_0(S)$ is obtained from the static quadrupole moments and $Q_0(B)$, from the $B(E2)$'s. In the simple rotational model, this ratio would equal unity, and in the harmonic vibrator model, it would equal zero.

There have been tests of this ratio in other models such as the Skyrme Hartree–Fock model by Bender et al. [2, 3]. This same model has been used to test the systematics of quadrupole deformations by Jaqaman and Zamick [4], Zheng et al. [5], Retamosa et al. [6, 7], and more recently by Sagawa et al. [8]. At the same time as Ref. [1], there appeared an article on the same topic but with a different approach by S.M. Lenzi et al. [9] and, more recently, by G. Thiamova et al. [10]. Very recent references [11, 12] show ever increasing interest in this subject.

In another vein, random interaction studies were performed by Velázquez et al. [13] and by Zelevinsky and Volya [14]. They found two spikes (i.e., high probabilities) in the Alaga ratio $A = 5Q^2/[16\pi B(E2)_{0\to 2}]$ at $A = 0$ and $A = A_0 = 4/49$, which can be associated with the vibrational and rotational limits, respectively.

On the other hand, for the nuclei that we considered in Ref. [1], the experimental ratio $Q_0(S)/Q_0(B)$ was, for the most part, large, sometimes exceeding one, e.g., for ^{20}Ne and ^{50}Cr. The one exception was ^{40}Ar, where the ratio was 0.06.

We would like to mention that Poves et al. [15] have shown that, in a full fp space, one gets a quasi-rotational band in ^{48}Cr. The spectrum is not $I(I + 1)$ exactly but there are strong intraband $E2$ transitions between the levels.

In this work, we shall extend this study by considering states of higher angular momentum as well. All calculations have been done using the shell-model code ANTOINE [16].

We define

$$R_{SB} = \frac{Q_0(S)_{I=2}}{Q_0(B)_{2\to 0}} = -\frac{7}{2\sqrt{16\pi}} \frac{Q(2^+)}{\sqrt{B(E2)_{2\to 0}}} = -0.4936659 \frac{Q(2^+)}{\sqrt{B(E2)_{2\to 0}}} \, , \qquad (1)$$

and

$$M(Q)_I = \frac{Q_0(S)_I}{Q_0(S)_2} = \frac{2}{7} \frac{2I + 3}{I} \frac{Q(I)}{Q(2)} \, , \qquad (2)$$

2

where $Q(I)$ is the (laboratory) static quadrupole moment of a state of angular momentum I. Note that the Alaga ratio mentioned above is $A = \frac{4}{49}|R_{SB}(2)|^2$.

We also define

$$M(B)_{I \to I-2} = \frac{Q_0(B)_{I \to I-2}}{Q_0(B)_{2 \to 0}} \ . \tag{3}$$

Now for a $K = 0$ rotational band, we have

$$B(E2)_{I \to I-2} = \frac{5}{16\pi}(I200|I-2,0)^2 Q_B^2(I) \ , \tag{4}$$

$$B(E2)_{2 \to 0} = \frac{5}{16\pi}\frac{Q_B^2(2)}{5} \ . \tag{5}$$

Hence,

$$M(B)_{I \to I-2}^2 = \frac{2}{15}\frac{(2I-1)(2I+1)}{I(I-1)}\frac{B(E2)_{I \to I-2}}{B(E2)_{2 \to 0}} \ . \tag{6}$$

Note that both $M(Q)_2$ and $M(B)_{2 \to 0}$ are equal to 1 by definition.

II. PRELIMINARY REMARKS

A. The Schematic Surface Delta Interaction

In the past, schematic models, despite giving somewhat oversimplified descriptions of the structures of nuclei, proved to be invaluable in casting insights into the trends of nuclear structure. As an example, Elliott's SU(3) model showed how one could approach rotational-model spectra in the Shell Model [17]. This was shown with a two-body momentum-dependant long-range quadrupole-quadrupole interaction and did not include the effects of spin-orbit splitting. Indeed, SU(3) models emanating from this interaction are emphasized in Refs. [9, 10].

In this work, the main thrust will be to use a realistic interaction with correct single particle splittings. However, since our results for R_{SB} agree with the rotational model even when the spectra are not rotational, we are motivated to get insight into this result by using a different schematic interaction, one which does not have $I(I+1)$ spectra but still exhibit collective behaviour. In contrast to Elliott's long range interaction [17], we will use the surface delta interaction of Moszkowski with degenerate single particle energies [18].

In Fig. 1, we show the calculated spectrum of ^{48}Ti with a surface delta interaction as compared with the $I(I+1)$ rotational spectrum. The parameters have been adjusted so that

3

the excitation energies of the first 2^+ states are the same. The rotational spectrum is more spread out but the surface delta spectrum still has rotational features and the spectrum is actually closer to the truth than the $I(I+1)$, at least for ^{48}Ti. Hence, the surface delta interaction will serve as a good counterpoint to the more realistic interaction considered in the next section.
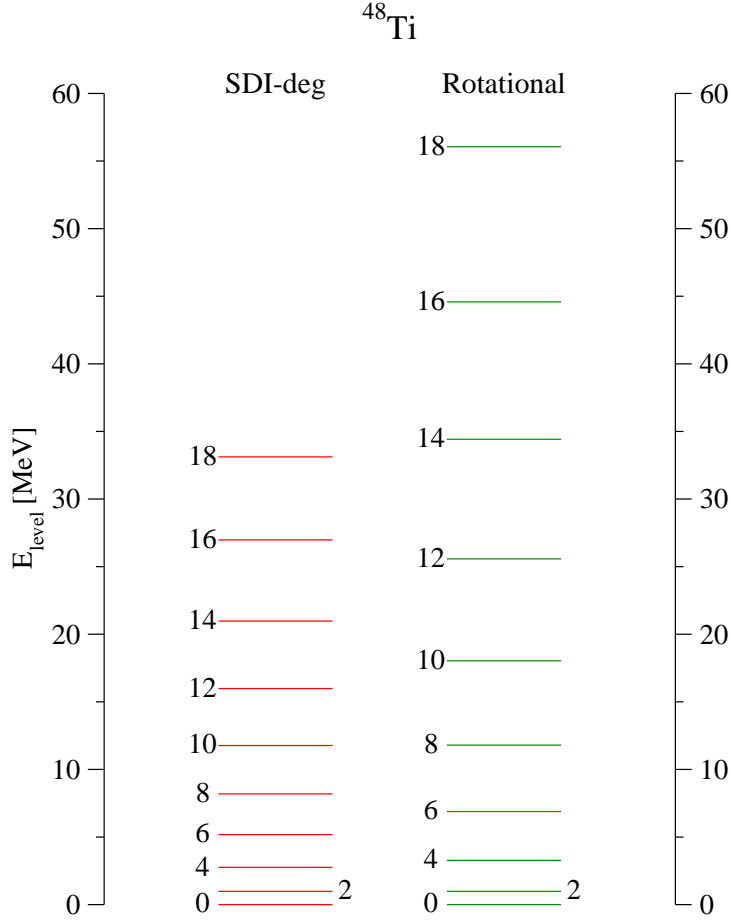

FIG. 1: Comparison of the SDI-deg and rotational $I(I+1)$ spectra for ^{48}Ti. Both interactions have been fitted to reproduce the experimental splitting of the 0_1^+ and 2_1^+ states.

B. Experimental Comparison

In Ref. [9], S.M. Lenzi et al. compare the $B(E2)$'s of $N = Z$ nuclei, ^{44}Ti and ^{48}Cr, with the SU(3) model of Elliott [17], making use of the momentum-dependent quadrupole-quadrupole interaction. Although the SU(3) model gives a rotational spectrum, the $BE(2)$'s do not follow the rotational formula. Rather, with increasing J, they decrease relative to the rotational formula. The authors make the point that, despite the absence of spin-orbit splitting, the SU(3) results are not too bad compared with experiment. For ^{48}Cr they refer to the experiments of Brandolini et al. [19]. We shall also use this reference for our analysis of $Q_0(B)_{I \to I-2}/Q_0(B)_{2 \to 0}$.

In tables I and II we can see the results from Ref. [19] for ^{48}Cr and ^{50}Cr, respectively. Note that, in the case of ^{48}Cr, $M(B)_{I \to I-2}$ decreases almost linearly with I. There is more experimental information, but, beyond the results shown in the tables, things get lost in band crossing.

TABLE I: Experimental $B(E2)$'s [e^2 fm^4] and ratio $M(B)_{I \to I-2}$ (see text) for ^{48}Cr; experimental data are taken from Ref. [19], except the $B(E2)_{2 \to 0}$, which is taken from Ref. [20].

	$B(E2)_{\text{exp}}$ [e^2 fm^4]	$M(B)_{I \to I-2}$
$2 \to 0$	272	1.00000
$4 \to 2$	329(110)	0.92016
$6 \to 4$	301(78)	0.83863
$8 \to 6$	230(69)	0.71651
$10 \to 8$	195(54)	0.65098
$12 \to 10$	167(25)	0.59716
$14 \to 12$	105(18)	0.47057
$16 \to 14$	37(8)	0.27805

III. RESULTS

As in Ref. [1], in Table III we check the relationship between the $B(E2)_{2_1^+ \to 0_1^+}$ and the static quadrupole moment $Q(2_1^+)$.

TABLE II: Same as Table I but for ^{50}Cr.

	$B(E2)_{\text{exp}}$ [e^2 fm^4]	$M(B)_{I \to I-2}$
$2 \to 0$	216	1.00000
$4 \to 2$	204(57)	0.81309
$6 \to 4$	235(47)	0.83154
$8 \to 6$	205(51)	0.75909
$10(1) \to 8$	72(14)	0.44389
$10(2) \to 8$	131(26)	0.59875

TABLE III: $Q(2^+)$ [e fm^2], $B(E2)_{2^+ \to 0^+}$ [e^2 fm^4], and R_{SB} for ^{44,46,48}Ti and ^{48,50}Cr obtained from a full fp shell calculation with the interactions SDI and FPD6.

	SDI-deg			FPD6		
	$Q(2^+)$	$B(E2) \downarrow$	R_{SB}	$Q(2^+)$	$B(E2) \downarrow$	R_{SB}
^{44}Ti	-26.319	165.74	1.0092	-20.156	121.45	0.9029
^{46}Ti	-29.349	206.06	1.0093	-22.071	136.41	0.9329
^{48}Ti	-32.337	247.38	1.0149	-17.714	112.16	0.8257
^{48}Cr	-37.936	377.60	0.9638	-33.271	275.68	0.9892
^{50}Cr	-41.681	435.82	0.9856	-30.955	243.80	0.9787

In the rotational model,

$$Q(2_1^+) = -\frac{2}{7}Q_0(S) \ , \tag{7}$$

$$B(E2)_{2_1^+ \to 0_1^+} = \frac{Q_0(B)^2}{16\pi} \ . \tag{8}$$

Furthermore, the ratio $R_{SB} = Q_0(S)/Q_0(B)$ should equal 1.

In Table III we give R_{SB} for two models: a surface delta interaction with degenerate single-particle energies (SDI-deg) and the more realistic calculation with the FPD6 interaction including single-particle energy splittings, both in a full fp space. The strength of the SDI-deg interaction was chosen to fit the experimental excitation energy of the 2_1^+ state. The nuclei considered are ^{44}Ti, ^{46}Ti, ^{48}Ti, ^{48}Cr, and ^{50}Cr. Note that, from Figs. 2–6, neither SDI-

6

deg or FPD6 have pure rotational spectra, although SDI is closer to a rotational spectrum, undoubtedly due to the fact that there are no single-particle splittings.
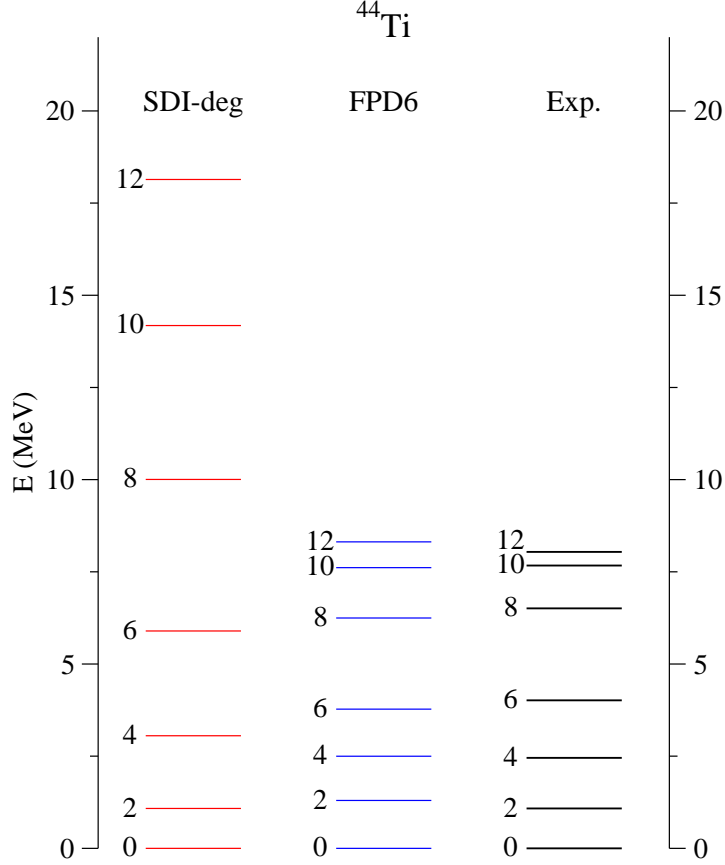

FIG. 2: Full fp space calculations of even-J states in ^{44}Ti with the SDI-deg and FPD6 interactions, and comparison with experiment.

The SDI-deg results for R_{SB} are remarkably close to unity, ranging from 0.964 to 1.009. With FPD6, the results range from 0.826 to 0.989—somewhat farther from unity, but again noticeably close. Remember that, in a very simple model for a vibrational nucleus, the ratio of R_{SB} would be zero. Clearly the shell model shows greater resistence for the intrinsic quadrupole moment $Q_0(S)$ to become small, as we might be led to believe from collective arguments.

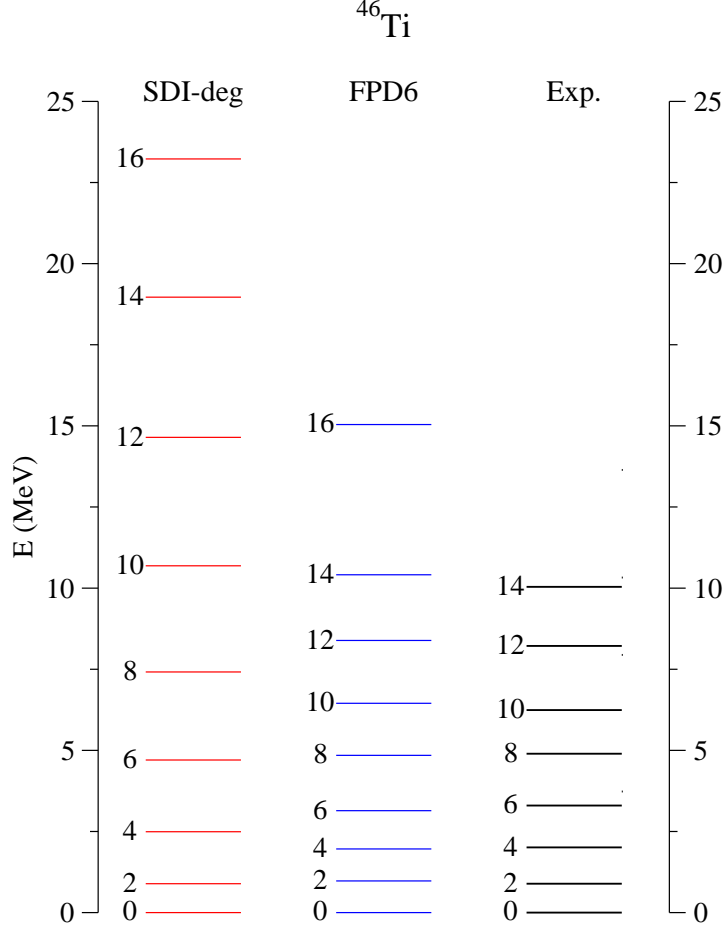In Tables IV–VIII, we show the results of $M(Q)_I$ and $M(B)_{I \to I-2}$ for all the nuclei with

FIG. 3: The same as Fig. 2 for ^{46}Ti.

both interactions. We first look at $M(Q)_I$ for the surface delta interaction. For ^{44}Ti, ^{46}Ti, and ^{48}Ti, the values are slightly larger but remarkably close to unity, even for very high spins, e.g., $I = 12, 16$, and 18 for $A = 44, 46$, and 48, respectively. In ^{48}Cr the results are not so close beyond $I = 6$, the values being 0.859, 0.766, and 0.779 for $I = 8, 10$, and 12_1. Strangely, for ^{50}Cr the results are better up to $I = 10$. All in all, though, we are very far away from the simple vibrational limit of zero.

If we look at $M(B)_{I \to I-2}$ with SDI-deg, the results up to the transition $8 \to 6$ are all greater than 0.8 and less than unity for all nuclei considered. Beyond that, there are some lower results that may be due to band crossing, e.g., the value of $M(B)_{12_1 \to 10_1}$ in ^{46}Ti is 0.0044; however, $M(B)_{12_2 \to 10_1}$ is 0.6654.
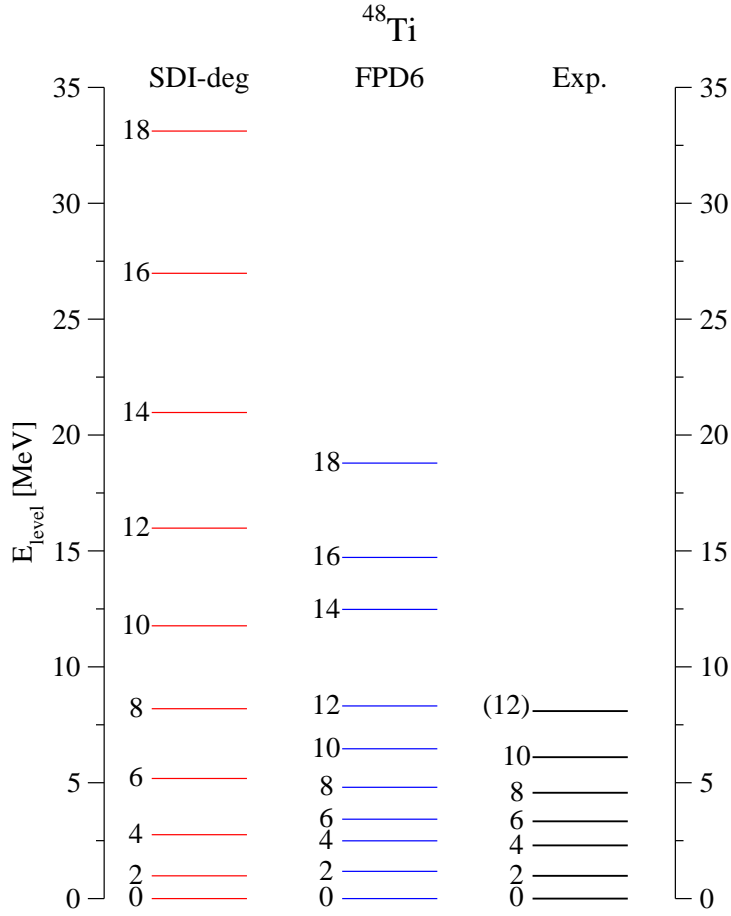
FIG. 4: The same as Fig. 2 for ^{48}Ti.

Results for the more realistic FPD6 interaction including single-particle energies are also shown in Tables IV–VIII. The results are over all not as close to unity as with SDI-deg. Still, one gets some substantial static quadrupole moments. Sometimes, the lowest state of a given angular momentum does not belong to a $K = 0$ band, e.g., the $I = 6_1^+$ state in ^{48}Ti or the 10_1^+ state in ^{50}Cr. The sign of the static quadrupole moment is opposite to what one would get assuming $K = 0$. In ^{48}Ti, the second 6^+ state fits better into this profile. The near degeneracies of the 6_1^+ and 6_2^+ states in ^{48}Ti has been discussed previously [21].

In previous works on ^{50}Cr [22, 23], it was noted that the first 10^+ state did not belong to the $K = 0$ ground state band. Indeed, if one must choose a K value, it would seem $K = 10$ is the best for the 10_1^+ state. This is supported by the fact that the static quadrupole moment
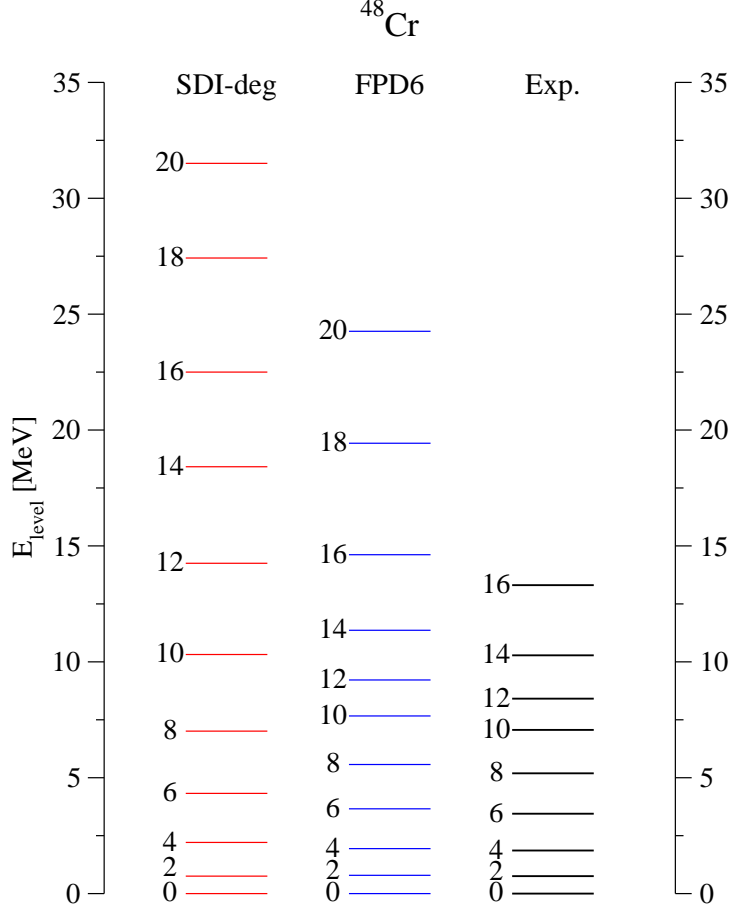
FIG. 5: The same as Fig. 2 for ^{48}Cr.

is large and positive, while the $K = 0$ static moments are negative. Moreover, if it were strictly $K = 10$ and the 8_1^+ were strictly $K = 0$, the $B(E2)$ would be strongly inhibited. The small value of $M(B)_{10_1 \to 8} = 0.2678$ somewhat supports this. The decay $10_2^+ \to 8_1^+$ is stronger, with $M(B)_{10_2 \to 8} = 0.6599$.

Let us briefly discuss Figs. 2–6 corresponding to ^{44}Ti, ^{46}Ti, ^{48}Ti, ^{48}Cr, and ^{50}Cr, respectively. Although not perfect, the FPD6 interaction in a full fp space yields a pretty good agreement for the energy levels of all nuclei here considered. The SDI interaction, for which the 0–2 splitting is fitted to experiment, gives a more spread out spectrum. It is closer to an $I(I + 1)$ spectrum than results with FPD6, but still significantly different. The spreading of the spectrum with SDI-deg is mainly due to the fact that there are no single-particle
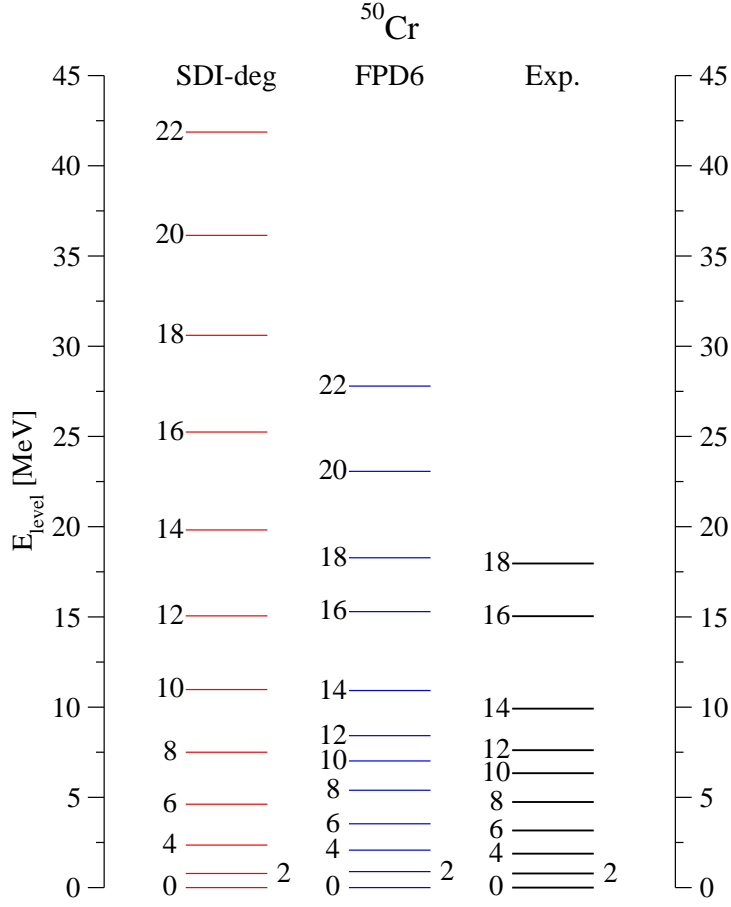
FIG. 6: The same as Fig. 2 for ^{50}Cr.

splittings in this model, i.e., $\epsilon_{f_{7/2}} = \epsilon_{f_{5/2}} = \epsilon_{p_{3/2}} = \epsilon_{p_{1/2}}$.

Just to give some numbers, in ^{48}Ti the experimental energy of the 12_1^+ state is 8.09 MeV, FPD6 gives 8.31 MeV, and SDI-deg gives 15.98 MeV. Using the simple rotational model and fitting the 0–2 splitting to experiment, the 12_1^+ state would, with an $I(I+1)$ spectrum, be at 25.57 MeV.

IV. THE HARMONIC VIBRATOR

In the harmonic vibrator model, the nuclear shape oscillates between oblate and prolate. One gets equally spaced spectra, i.e., the ground state has angular momentum $I = 0$, the

TABLE IV: Ratios of intrinsic quadrupole moments $M(Q)_I$ and $M(B)_{I \to I-2}$ (see text) for ^{44}Ti using both SDI-deg and FPD6 interactions.

$I \to I-2$	SDI-deg		FPD6	
	$M(Q)_I$	$M(B)_{I \to I-2}$	$M(Q)_I$	$M(B)_{I \to I-2}$
$2 \to 0$	1	1	1	1
$4 \to 2$	1.0092	0.9741	1.0534	0.9764
$6 \to 4$	1.0176	0.9096	1.1047	0.8554
$8 \to 6$	1.0276	0.8241	0.8498	0.6971
$10 \to 8$	1.0406	0.7239	0.7800	0.6802
$12 \to 10$	1.0556	0.5498	0.8472	0.5130

TABLE V: The same as Table IV for ^{46}Ti.

$I \to I-2$	SDI-deg		FPD6	
	$M(Q)_I$	$M(B)_{I \to I-2}$	$M(Q)_I$	$M(B)_{I \to I-2}$
$2 \to 0$	1	1	1	1
$4 \to 2$	1.0159	0.9878	1.0349	0.9975
$6 \to 4$	1.0328	0.9351	0.9483	0.9398
$8 \to 6$	1.0295	0.8152	0.9522	0.8626
$10 \to 8$	1.0270	0.7562	0.9362	0.7436
$12_1 \to 10$	1.0131	0.0044	0.6763	0.4493
$12_2 \to 10$	1.0658	0.6654	0.2357	0.2245
$14 \to 12_1$	1.0331	0.6803	0.6724	0.3804
$14 \to 12_2$	$''$	0.0007	$''$	0.2709
$16 \to 14$	1.0480	0.5212	0.8911	0.0644

first excited state has angular momentum $I = 2$ and energy $E(2)$. At $2E(2)$ there are states with $I = 0, 2$, and 4; at $3E(2)$ there are states with $I = 0, 2, 3, 4$, and 6; etc.

The selection rules and $B(E2)$'s relations are given in Bohr and Mottelson vol. 2, page

TABLE VI: The same as Table IV for ^{48}Ti.

$I \rightarrow I-2$	SDI-deg		FPD6	
	$M(Q)_I$	$M(B)_{I \rightarrow I-2}$	$M(Q)_I$	$M(B)_{I \rightarrow I-2}$
$2 \rightarrow 0$	1	1	1	1
$4 \rightarrow 2$	1.0172	1.0015	0.8654	1.0310
$6_1 \rightarrow 4$	1.0276	0.9884	-0.8738	0.5016
$6_2 \rightarrow 4$	0.2782	0.0309	0.8041	0.7124
$8 \rightarrow 6_1$	1.0319	0.9598	0.6134	0.5768
$8 \rightarrow 6_2$	''	0.0016	''	0.3832
$10 \rightarrow 8$	1.0340	0.9193	0.8153	0.5682
$12 \rightarrow 10$	1.0347	0.8589	0.5462	0.3616
$14 \rightarrow 12$	1.0392	0.7821	0.8447	0.1491
$16 \rightarrow 14$	1.0519	0.6657	0.9128	0.4386
$18 \rightarrow 16$	1.0614	0.5062	1.0951	0.0646

349 [24]. The equations for a transition are

$$\sum_{\zeta_{n-1} I_{n-1}} B(E\lambda; n_\lambda \zeta_n I_n \rightarrow n_{\lambda-1} \zeta_{n-1} I_{n-1}) = n_\lambda B(E\lambda, n_\lambda = 1 \rightarrow n_\lambda = 0) \ , \qquad (9)$$

i.e., there is stimulated emission—the more quanta there are, the bigger the $B(E\lambda)$. In the above, n_λ is the number of vibrational quanta, I_n is the angular momentum and ζ_n stands for any additional quantum numbers. Bohr and Mottelson also give the selection rule $\Delta n_\lambda = \pm 1$, which implies that static quadrupole moments vanish, consistent with the opening sentence in this section [24].

Since we are considering transitions from a state with the maximum angular momentum ($I_{\max}$) of all degenerate states with n_λ quanta, the final state for $E2$ transitions must have $I = I_{\max} - 2$, so there is only one term in the left-hand side: $I_{\max} - 2$. Note that $n_\lambda = I_{\max}/2$

$$B(E2)_{I \rightarrow I-2} = \frac{I}{2} B(E2)_{2 \rightarrow 0} \ . \qquad (10)$$

Hence, we obtain

$$M_{\text{vib}}(B)_{I \rightarrow I-2} = \left(\frac{1}{15} \frac{(2I-1)(2I+1)}{I-1} \right)^{1/2} \ . \qquad (11)$$

13

TABLE VII: The same as Table IV for ^{48}Cr.

$I \to I-2$	SDI-deg		FPD6	
	$M(Q)_I$	$M(B)_{I \to I-2}$	$M(Q)_I$	$M(B)_{I \to I-2}$
$2 \to 0$	1	1	1	1
$4 \to 2$	0.9797	0.9998	1.0088	0.9887
$6 \to 4$	0.9028	0.9851	0.9679	0.9600
$8 \to 6$	0.8586	0.9592	0.9370	0.9101
$10 \to 8$	0.7660	0.9121	0.7703	0.8028
$12_1 \to 10$	0.7788	0.8839	0.1381	0.5277
$12_2 \to 10$	1.3175	0.0985	0.5786	0.5102
$14_1 \to 12_1$	1.3722	0.0790	0.1675	0.5024
$14_2 \to 12_1$	0.7588	0.8642	0.6645	0.1394
$16_1 \to 14_1$	1.4145	0.4311	0.1537	0.3536
$16_2 \to 14_1$	0.7379	0.1255	0.6231	0.1401
$16_2 \to 14_2$	″	0.6032	″	0.5163
$18_1 \to 16_1$	1.1348	0.0000	0.5938	0.0577
$18_1 \to 16_2$	″	0.0000	″	0.4369
$18_2 \to 16_1$	0.8025	0.0000	0.7394	0.0157
$18_2 \to 16_2$	″	0.5765	″	0.1430
$20 \to 18$	1.0753	0.4473	0.8097	0.1183

Note that $M(B)_{I \to I-2}$ increases steadily with I, which is not the case with SDI-deg or FPD6. Some values of $M_{\text{vib}}(B)_{I \to I-2}$ for $I = 0, 2, 4, 6, 8$, and 10 are, respectively, $1, 1.183, 1.381, 1.558, 1.719$, and 1.867. For large values of I, we have

$$M(B)_{I \to I-2} \to \left(\frac{4}{15} I \right)^{1/2} , \tag{12}$$

still growing steadily with I.

As mentioned before, the vibrational prediction for static quadrupole moments is $M_{\text{vib}}(Q)_I = 0$, which is certainly not the case with SDI-deg or FPD6.

TABLE VIII: The same as Table IV for ^{50}Cr.

$I \rightarrow I-2$	SDI-deg		FPD6	
	$M(Q)_I$	$M(B)_{I \rightarrow I-2}$	$M(Q)_I$	$M(B)_{I \rightarrow I-2}$
$2 \rightarrow 0$	1	1	1	1
$4 \rightarrow 2$	0.9881	1.0027	1.0014	1.0074
$6 \rightarrow 4$	0.9631	0.9954	0.5587	0.8785
$8 \rightarrow 6$	0.9332	0.9807	0.6464	0.8154
$10_1 \rightarrow 8$	0.9064	0.9557	-0.9601	0.2678
$10_2 \rightarrow 8$	1.0923	0.0094	0.2300	0.6599
$12_1 \rightarrow 10_1$	0.8857	0.9751	-0.3819	0.3115
$12_1 \rightarrow 10_2$	"	0.0959	"	0.2502
$12_2 \rightarrow 10_1$	1.1533	0.0058	0.5044	0.1502
$12_2 \rightarrow 10_2$	"	0.8039	"	0.5064
$14_1 \rightarrow 12_1$	0.8482	0.8672	-0.2057	0.3662
$14_1 \rightarrow 12_2$	"	0.1310	"	0.1013
$14_2 \rightarrow 12_1$	1.1224	0.0131	0.3175	0.0947
$14_2 \rightarrow 12_2$	"	0.1404	"	0.4982
$16 \rightarrow 14_1$	0.8832	0.8584	0.2218	0.0943
$16 \rightarrow 14_2$	"	0.0161	"	0.5892
$18 \rightarrow 16$	1.1256	0.0266	0.1888	0.4213
$20 \rightarrow 18$	1.1306	0.6272	0.5944	0.0619
$22 \rightarrow 20$	1.0694	0.4435	0.9263	0.1189

V. CLOSING REMARKS

This work is an extension of previous work by Robinson et al [1], where it was noted that, for a large variety of nuclei, the simple rotational formula, if fitted to the experimental $B(E2)$ from the ground state to the 2_1^+ state, could give a good result for the static quadruple moment of the 2_1^+ state, i.e., in the notation of this work, R_{SB} is close to one. The one exception is ^{40}Ar.

In this work, we extend the calculations to higher energy and higher angular momentum. We use both a phenomenological interaction FPD6 with realistic single-particle splittings, and, as a counterpoint to $Q \cdot Q$, we use the schematic surface delta interaction. We claim the latter shows also collective properties. As seen in Fig. 1, its spectrum is not rotational but it does have features that many nuclei possess—a collective appearance; and it should be noted that the nuclei we consider do not have rotational spectra either. We do not include single-particle splittings in SDI, and this is the main reason, rather than the SDI per se, that the spectrum, though less spread out than in the rotational model, is more spread out than with a realistic interaction or, indeed, experiment. The effects of single-particle splittings are taken care of in the realistic case.

The results with SDI for $M(Q)_I$ (ratios of intrinsic quadrupole moments) is close to one for many nuclei and many angular momenta I. One only runs into trouble when one has near degeneracies like 6_1^+ and 6_2^+ in ^{48}Ti, as well as 10_1^+ and 10_2^+ in ^{50}Cr. These degeneracies have been addressed previously by Zamick et al. [21, 22, 23]. And when one gets band crossings, the situation can get confused.

But still, all in all, with SDI we get some remarkable agreements with the rotational formulas for ratios between static quadrupole moments and $B(E2)$'s, not only for angular momentum $I = 2$, but for higher I as well. The realistic interactions also yield similar results, although perhaps not quite as definitive as does the schematic SDI.

[1] S.J.Q. Robinson, A. Escuderos, L. Zamick, P. von Neumann-Cosel, A. Richter, and R.W. Fearick, Phys. Rev. C **73**, 037306 (2006).

[2] M. Bender, H. Flocard, and P.-H. Heenen, Phys. Rev. C **68**, 044321 (2003).

[3] M. Bender, P. Bonche, T. Duguet, and P.-H. Heenen, Phys. Rev. C **69**, 064303 (2004).

[4] H. R. Jaqaman and L. Zamick, Phys. Rev. C **30**, 1719 (1984).

[5] D. C. Zheng, D. Berdichevsky, and L. Zamick, Phys. Rev. C **38**, 437 (1988).

[6] J. Retamosa, J. M. Udías, A. Poves, and E. Moya de Guerra, Nucl. Phys. A **511**, 221 (1990).

[7] A. Poves, J. Retamosa, and E. Moya de Guerra, Phys. Rev. C **39**, 1639 (1989); A. Poves and E. Moya de Guerra, in Proc. Int. Seminar, *Shell model and nuclear structure: where do we stand?*, ed. A. Covello (World Scientific, Singapore, 1989) p. 283.

[8] H. Sagawa, X.R. Zhou, and X.Z. Zhang, Phys. Rev. C **72**, 054311 (2005).

[9] S.M. Lenzi, E.E. Maqueda, and P. von Brentano, Eur. Phys. J. A **27**, 341 (2006).

[10] G. Thiamova, D.J. Rowe, and J.L. Wood, Nucl. Phys. A **780**, 112 (2006).

[11] B. Sabbey, M. Bender, G.F. Bertsch, and P.-H. Heenen, Phys. Rev. C **75**, 044305 (2007).

[12] G.F. Bertsch, M. Girod, S. Hilaire, J.-P. Delaroche, H. Goutte, and S. Péru, arXiv:nucl-th/0701037v1 (2007).

[13] V. Velázquez, J. G. Hirsch, A. Frank, and A. P. Zuker, Phys. Rev. C **67**, 034311 (2003).

[14] V. Zelevinsky and A. Volya, Phys. Rep. **391**, 311 (2004).

[15] E. Caurier, A.P. Zuker, A. Poves, and G. Martínez-Pinedo, Phys. Rev. C **50**, 225 (1994).

[16] E. Caurier, shell-model code ANTOINE, IRES, Strasbourg (1989–2004); E. Caurier and F. Nowacki, Acta Phys. Pol. **30**, 705 (1999).

[17] J.P. Elliott, Proc. Roy. Soc. London A **345**, 128 and 252 (1958).

[18] I.M. Green and S.A. Moszkowski, Phys. Rev. **139**, B790 (1965).

[19] E. Brandolini et al., Nucl. Phys. A **642**, 387 (1998).

[20] S. Raman, C.W. Nestor, Jr., and P. Tikkanen, At. Data Nucl. Data Tables **78**, 1 (2001).

[21] S.J.Q. Robinson and L. Zamick, Phys. Rev. C **63**, 057301 (2001).

[22] L. Zamick, M. Fayache, and D.C. Zheng, Phys. Rev. C **53**, 188 (1996).

[23] L. Zamick and D.C. Zheng, Phys. Rev. C **54**, 956 (1996).

[24] A. Bohr and B.R. Mottelson, *Nuclear Structure, Vol. II Nuclear Deformation* (W.A. Benjamin Inc., Reading, Mass., 1975).